Inorg. Chem. **2002**, *41*, 5760–5769

Kinetic, Mechanistic, and DFT Study of the Electrophilic Reactions of Nitrosyl Complexes with Hydroxide

Federico Roncaroli,[†] Mara E. Ruggiero,[‡] Douglas W. Franco,[‡] Guillermina L. Estiú,*[,†,§] and José A. Olabe*[,†]

Departamento de Química Inorgánica, Analítica y Química Física, INQUIMAE, Facultad de Ciencias Exactas y Naturales, Universidad de Buenos Aires, Pabellón 2, Ciudad Universitaria, Buenos Aires C1428EHA, Argentina, Departamento de Química, CEQUINOR, Facultad de Ciencias Exactas, Universidad Nacional de La Plata, La Plata, Argentina, and Instituto de Química de Sao Carlos, USP, Sao Carlos, Brasil

Received April 15, 2002

We present a kinetic study of OH^- additions to several nitrosyl complexes containing mainly ruthenium and different coligands (polypyridines, amines, pyridines, cyanides). According to a first-order rate law in each reactant, we propose a fast ion pair formation equilibrium, followed by addition of OH^- to the $[MX_5NO]^n$ moieties, with formation of the $[MX_5NO_2H]^{(n-1)}$ intermediates. Additional attack by a second OH^- gives the final products, $[MX_5NO_2]^{(n-2)}$. A linear plot was found for ln k_4 (the addition rate constant) against the redox potential for nitrosyl reduction, $E_{NO^+/NO}$, showing a free-energy relationship with a slope close to 20 V^{-1}, consistent with an associative mechanism. Theoretical DFT calculated descriptors, as the charge density in the {MNO} moieties and the LUMO energies, qualitatively correlate with the rate constants. A linear to bent transformation was calculated for the nitrosyl complexes, as they evolve to the angular MNO_2H and MNO_2 complexes. The geometries were optimized for the different complexes and adduct-intermediates, showing significant changes in the relevant distances and angles upon OH^- addition. IR vibrations and electronic transitions were also calculated. The complete reaction profile was studied for the nitroprusside ion, including the description of the transition state structure. Experimental activation parameters revealed that both the activation enthalpies and entropies increase when going from the negatively charged to the positively charged complexes. As the rate constants increase in the same direction, we conclude that the reactions are entropically driven, compensating, this function, the increase in the activation enthalpies. The latter trend can be explained by the energies involved in angular reorganization after OH^- coordination, which are larger as the positive charge in the nitrosyl moiety becomes larger. The use of $E_{NO^+/NO}$ as a predictive tool for electrophilic reactivity could be extended to similar reactions implying other nucleophiles, such as amines and thiolates.

Introduction

The electrophilic reactions of the nitrosyl ligand bonded to transition metal centers have been known for a long time and constitute one of its most important reactivity modes.[1] Early use of the reactions of the pentacyanonitrosylferrate(II) ion, $[Fe(CN)_5NO]^{2-}$, (NP) as color tests for identifying SH^- or SO_3^{2-},[2] have been followed by mechanistic studies in the 1970s.[3] The work has been extended to other $\{MX_5NO\}^n$ complexes (mainly ruthenium with ancillary coligands such as amines, polypyridines, etc.).[4] These systems generally have the {MNO}[6] configuration, according to the Enemark–Feltham notation,[5] the superscript meaning the number of electrons associated with the metal d and π^*(NO) orbitals.

Several nucleophiles have been used in these studies. Most important are the N-binding and S-binding species: ammonia, amines, hydroxylamine, hydrazine, azide, SH^-, SR^-,

* To whom correspondence should be addressed. E-mail: olabe@qi.fcen.uba.ar (J.A.O.), estiu@biol.unlp.edu.ar (G.L.E.).
† Universidad de Buenos Aires.
§ Universidad Nacional de La Plata.
‡ Instituto de Química de Sao Carlos.

(1) Richter-Addo, G. B.; Legzdins, P. *Metal Nitrosyls*; Oxford University Press: New York, 1992.
(2) Swinehart, J. H. *Coord. Chem. Rev.* **1967**, *2*, 385.
(3) McCleverty, J. A. *Chem. Rev.* **1979**, *79*, 53−76.
(4) (a) Bottomley, F. In *Reactions of Coordinated Ligands, Vol. 2*; Braterman, P. S., Ed.; Plenum: New York, 1985; p 115. (b) Ford, P. C.; Lorkovic, I. M. *Chem. Rev.* **2002**, *102*, 993.
(5) Enemark, J. H.; Feltham, R. D. *Coord. Chem. Rev.* **1974**, *13*, 339.

10.1021/ic025653q CCC: $22.00
Published on Web 10/09/2002

SO_3^{2-}, and so forth. Their reactions with the $\{MX_5NO\}^n$ fragments are assumed to proceed through initial reversible adduct formation and are followed by redox processes associated with the reduction of nitrosyl and oxidation of the nucleophile.[3,4] These reactions are most relevant in the redox interconversions of nitrite to ammonia in the natural media, which still show mechanistic uncertainties due to the lack of characterization of several intermediates, which are sometimes even ill-defined.[3,4,6] On the other hand, the electrophilicity of nitrosyl, particularly toward thiolates, is proposed to be important in the process of NO uptake, release, and transportation by transition metal centers in the biological fluids, given the presence of iron-containing enzymes which attain a pseudo-octahedral low-spin d^6 configuration upon NO binding.[7]

The simplest electrophilic reactions of bound nitrosyl are those involving OH^- as the nucleophile (eq 1), because no subsequent redox processes occur after addition. The stoichiometry is characteristic of several complexes with different MX_5 fragments (M = Fe(II), Ru(II), Os(II), Ir(III); X = NH_3, CN^-, halides, OH^-, polypyridines, etc.):[3,4]

$$[MX_5NO]^n + 2OH^- \rightleftharpoons [MX_5NO_2]^{(n-2)} + H_2O \quad K_{eq} \qquad (1)$$

In eq 1, a reversible acid−base reaction occurs. Although values of K_{eq} have been measured for a variety of MX_5 fragments, kinetic and mechanistic results are scarce, limited to reactions of the pentacyanonitrosylmetalates (Fe, Ru, Os).[2,8] It is generally accepted that slow OH^- addition to the {MNO} fragment is followed by a fast deprotonation of the $\{MX_5NO_2H\}^{(n-1)}$ intermediates to give the corresponding nitro complexes. However, no direct evidence of these intermediates is available.

The electrophilic reactivity of bound nitrosyl was associated earlier with the value of the IR stretching frequency, ν_{NO}. It has been proposed that complexes with ν_{NO} = ca. 1860 cm^{-1} or greater will be reactive.[9] This is a useful guide with some rationale in that ν_{NO} should reflect the electron density at the N atom of the nitrosyl, which is the site of attack by nucleophiles.[3,4] It has also been recognized that larger values of K_{eq} are obtained with complexes having the more positive values of ν_{NO}.[10] However, these correlations are still unable to present a satisfactory account of the factors determining the reactivity of bound nitrosyl, given the variety of metal centers, ancillary X ligands, and overall charge of the complexes. Remarkably, electrophilic reactivity is currently discussed in terms of the above-mentioned parameters, but the key ones are lacking, namely, the values of the *rate constants* for the elementary steps comprising nucleophilic addition.[3,4]

We present a systematic kinetic and mechanistic study of the reactions of $\{MX_5NO\}^n$ complexes with OH^- (mainly ruthenium metal centers). Included are the members of well characterized series of nitrosyl complexes, containing a variety of ancillary ligands, for which some types of information already exist, such as K_{eq}, ν_{NO}, and $E_{NO^+/NO}$ values. To better understand the influence of different electronic/structural factors on the electrophilic reactivity of the metal nitrosyl complexes, looking at the same time for descriptors of predictive value, density functional calculations have been performed for representative members of the series. These calculations have been also applied to the characterization of the reaction intermediates of reaction 1, focusing on NP for a more detailed analysis of the associated mechanism.

Experimental Section

Preparation of Complexes. The complexes of the *cis*-$[Ru(bpy)_2(NO)(X)]^{n+}$ series were prepared as previously described, for X = AcN, NO_2^-, Cl^-,[10ab] as was also the case with *cis*-$[Ru(bpy)(trpy)(NO)]^{3+}$.[10c] The complexes of the *trans*-$[Ru(NO)(py)_4X)]^{2+}$ series (X = Cl^-, OH^-) were obtained as reported previously,[11] and the one with X = NCS^- was prepared by a similar technique. The synthesis of *trans*-$[(NC)Ru(py)_4CNRu(py)_4(NO)]^{3+}$ has been recently published.[12] The members of the *trans*-$[Ru(NH_3)_4(NO)(X)]^{n+}$ series (X = pyrazine, nicotinamide, chloropyridine, pyridine, 4-methylpyridine, and histidine) were prepared as described in the literature.[13,14] The purity was checked by ^1H NMR, IR, and UV−vis spectroscopies. All chemicals used for buffer solutions were analytical grade and were used without further purification.

Spectroscopic, Electrochemical, and Kinetic Measurements. IR spectra were taken in KBr pellets on a Thermo Nicolet model Avatar 320 FT-IR instrument. ^1H NMR spectra were obtained on a Bruker 500 MHz spectrometer. Electrochemical studies were done with all the complexes, with the exception of the pentacyanonitrosylmetalates (data taken from the literature),[15] on a Princeton Applied Research potentiostat 273A, using square wave voltammetry (SWV) at 60 Hz, vitreous carbon as working electrode, and Ag/AgCl (3 M KCl) as a reference. The electrolyte was a HCl solution, pH 2.0 at I = 1 M (NaCl).

All the kinetic experiments were done at I = 1 M (NaCl), with final complex concentration 2−5 mg/100 mL and under pseudo-first-order conditions. Buffer solutions (0.05 M) were employed to control the pH of the system (acetate buffer for pH 3.5−6.0, phosphate buffer for pH 6.0−8.0, and carbonate buffer for pH 8.0−10.0). At pH values higher than 11, NaOH solutions were used. Distilled water was boiled for plenty of time to eliminate carbon

(6) Averill, B. A. *Chem. Rev.* **1996**, *96*, 2951.
(7) (a) Butler, A. R.; Glidewell, C. *Chem. Soc. Rev.* **1987**, *16*, 361. (b) Clarke, M. J.; Gaul, J. B. *Struct. Bonding (Berlin)* **1993**, *81*, 147. (c) Stamler, J. S.; Singel, D. J.; Loscalzo, J. *Science* **1992**, *258*, 1898.
(8) (a) Swinehart, J. H.; Rock, P. A. *Inorg. Chem.* **1966**, *5*, 573. (b) Masek, J.; Wendt, H. *Inorg. Chim. Acta* **1969**, *3*, 455. (c) Chevalier, A. A.; Gentil, L. A.; Olabe, J. A. *J. Chem. Soc., Dalton Trans.* **1991**, 1959. (d) Baraldo, L. M.; Bessega, M. S.; Rigotti, G. E.; Olabe, J. A. *Inorg. Chem.* **1994**, *33*, 5890.
(9) Bottomley, F. *Acc. Chem. Res.* **1978**, *11*, 158.
(10) (a) Callahan, R. W.; Meyer, T. J. *Inorg. Chem.* **1977**, *16*, 574. (b) Nagao, H.; Nishimura, H.; Funato, H.; Ichikawa, Y.; Howell, F. S.; Mukaida, M.; Kakihana, H. *Inorg. Chem.* **1989**, *28*, 3955. (c) Pipes, D. W.; Meyer, T. J. *Inorg. Chem.* **1984**, *23*, 2466. (d) Godwin, J. N.; Meyer, T. J. *Inorg. Chem.* **1971**, *10*, 2150.
(11) Bottomley, F.; Mukaida, M. *J. Chem. Soc., Dalton Trans.* **1982**, 1933.
(12) Roncaroli, F.; Baraldo, L. M.; Slep, L. D.; Olabe, J. A. *Inorg. Chem.* **2002**, *41*, 1930.
(13) Gomes, M. G.; Davanzo, C. U.; Silva, S. C.; Lopes, L. G. F.; Santos, P. S.; Franco, D. W. *J. Chem. Soc., Dalton Trans.* **1998**, 601.
(14) (a) Borges, S.; Davanzo, C. U.; Castellano, E. E.; Schpector, J. Z.; Silva, S. C.; Franco, D. W. *Inorg. Chem.* **1998**, *37*, 2670. (b) Franco, D. W. Unpublished results.
(15) (a) Fiedler, J. *Collect. Czech. Chem. Commun.* **1993**, *58*, 461. (b) Baumann, F.; Kaim, W.; Baraldo, L. M.; Slep, L. D.; Olabe, J. A.; Fiedler, J. *Inorg. Chim. Acta* **1999**, *285*, 129.

dioxide and then was used to prepare NaOH solutions, which were handled under nitrogen. The concentration of OH^- was determined by titration with potassium biphthalate. The pH measurements were done with a Metrohm 744 pH meter, using Merck buffers for calibration.

The complex solution and the buffer or the NaOH solution were maintained at the desired temperature (±0.1 °C) with a RC 6 Lauda thermostat for 15 min and, then, were mixed by means of a RX1000 Applied Photophysics stopped-flow accessory, attached to a 1-cm quartz flow cell. Spectral changes in the range 200−800 nm were recorded with a Hewlett-Packard 8453 diode array spectrophotometer. Six wavelengths that showed the biggest changes were selected, and kinetic traces were obtained from them. Each experiment was repeated at least three times. All traces were fitted to one exponential until at least five half-lives, unless otherwise stated. This afforded at least 18 values for the observed rate constant (k_{obs}). Values which differed less than 10% (usually less than 5%) were averaged. Complexes **1**, **6**, **8**, and **14** did not show a first-order process during the reaction, and the whole spectral changes were analyzed by the SPECFIT program.[16] A two exponential model was employed, and the rate constant corresponding to the first process was considered as the observed rate constant (k_{obs}). Complex **8** was studied at [OH^-] lower than 1.7×10^{-2} M, because at higher concentrations the initial spectrum was different from the reagent spectrum, the process was a first-order one, and the observed rate constant was much lower.

The concentration of OH^- was varied at least 1 order of magnitude to get the second-order rate constant (k_{OH^-}). Plots of k_{obs}[OH^-] versus [OH^-]^2 were built for all the complexes. In all the cases, a linear distribution was observed. The slope was equal to the second-order rate constant, k_{OH^-}. Plots of k_{obs} versus [OH^-] showed linear distributions in most cases, and the slope did not differ significantly from the one obtained by the previous method. This procedure was repeated for selected systems at different temperatures (range 10−40 °C), and Eyring plots allowed for the activation parameters. For the estimation of K_{ip} (eq 3), a currently used electrostatic treatment was employed.[17] Distances of closest approach were estimated from crystalline structures of related compounds published in the Cambridge Structural Database.[18]

Computational Details. Density functional calculations have been done using Gaussian 98 (g98)[19] and the Becke three-parameter hybrid functional[20] with LYP correlation functional (B3LYP).[21] Different basis sets have been used to analyze the structural and electronic characteristics of the $\{MX_5NO\}^n$ complexes and the $\{MX_5NOOH\}^{(n-1)}$ addition products. The results obtained with the simplest split valence basis (3-21G)[22] have been compared with those derived from the use of double-ζ split valence plus polarization for the first row atoms (6-31G**),[23] combined with quasirelativistic electron core potentials (LANL2DZ,[24] SDD[25]) and the corresponding optimized sets of basis functions for the Fe and Ru centers. Self-consistent reaction field theory (SCRF)[26] has been used to calculate the effects of the solvent within the g98 calculations. In this approach, the reaction field component of the energy is incorporated directly in the Hamiltonian, and the molecular wave function is thus optimized in a manner that includes the solvation energy. Among the different schemes developed, the isodensity polarizable continuum model (IPCM)[27] has been used throughout the calculations. In this model, the gas-phase molecular wave function is used to define the solvent−solute interface, that is, the surface in which the dielectric constant abruptly goes to zero.

The complete reaction profile has been studied for the addition of OH^- to NP, using the same functional and double-ζ split valence plus polarization basis (6-31G**).[23] Transition state (TS) calculations followed a quadratic synchronous transit approach (QST2).[28] Time-dependent density functional theory (TDDFT)[29] was conducted to study the energies and intensities involved in single excitations of NP and its reaction products, including diffuse functions in the basis (6-31+G**). The reliability of this approach is well documented.[30] The nature of the singular points has been confirmed by means of harmonic frequency calculations in all the cases. The reported local density charges derive from a Mulliken population analysis.

Results and Discussion

Kinetic Results and Mechanistic Analysis. Table 1 displays the rate constants for the nucleophilic addition reactions of OH^- to the pentacyanonitrosylmetalates (Fe, Ru, Os),[8] as well as the values obtained in the present work for the rest of the $\{MX_5NO\}$ complexes. Also included are the corresponding values of ν_{NO}, $E_{NO^+/NO}$, and K_{eq}.

As a representative example, Figure 1 shows the successive spectra for the reaction of *trans*-$[Ru(4\text{-Mepy})(NH_3)_4(NO)]^{3+}$ with OH^-. The conversion of the nitrosyl complex to the *trans*-$[Ru(4\text{-Mepy})(NH_3)_4(NO_2)]^+$ product, according to eq 1, is revealed by the onset of the intense band at 378 nm, which may be assigned to a metal-to-ligand charge-transfer (MLCT) from Ru(II) to the nitro ligand. The isosbestic point

(16) (a) Binstead, R. A.; Zuberbuhler, A. D. *SPECFIT*; Spectrum Software Associates: Chapel Hill, NC, 1993−1999. (b) Zuberbuhler, A. D. *Anal. Chem*. **1990**, *62*, 2220.

(17) (a) Haim, A. *Comments Inorg. Chem*. **1985**, *4*, 113. (b) Miralles, A. J.; Szecsy, A. P.; Haim, A. *Inorg. Chem*. **1982**, *21*, 697. (c) Curtis, J. C.; Meyer, T. J. *Inorg. Chem*. **1982**, *21*, 1562.

(18) *Cambridge Structural Database System*, version 5.23; Cambridge Crystallographic Data Centre: Cambridge, U.K., 2001.

(19) Frisch, M. J.; Trucks, G. W.; Schlegel, H. B.; Scuseria, G. E.; Robb, M. A.; Cheeseman, J. R.; Zakrzewski, V. G.; Montgomery, J. A., Jr.; Stratmann, R. E.; Burant, J. C.; Dapprich, S.; Millam, J. M.; Daniels, A. D.; Kudin, K. N.; Strain, M. C.; Farkas, O.; Tomasi, J.; Barone, V.; Cossi, M.; Cammi, R.; Mennucci, B.; Pomelli, C.; Adamo, C.; Clifford, S.; Ochterski, J.; Petersson, G. A.; Ayala, P. Y.; Cui, Q.; Morokuma, K.; Malick, D. K.; Rabuck, A. D.; Raghavachari, K.; Foresman, J. B.; Cioslowski, J.; Ortiz, J. V.; Stefanov, B. B.; Liu, G.; Liashenko, A.; Piskorz, P.; Komaromi, I.; Gomperts, R.; Martin, R. L.; Fox, D. J.; Keith, T.; Al-Laham, M. A.; Peng, C. Y.; Nanayakkara, A.; Gonzalez, C.; Challacombe, M.; Gill, P. M. W.; Johnson, B. G.; Chen, W.; Wong, M. W.; Andres, J. L.; Head-Gordon, M.; Replogle, E. S.; Pople, J. A. *Gaussian 98*, Revision A. 9, Gaussian, Inc.: Pittsburgh, PA, 1998.

(20) Becke, A. D. *J. Chem. Phys*. **1993**, *98*, 5648.

(21) Lee, C.; Yang, W.; Parr, R. G. *Phys. Rev*. **1988**, *B37*, 785.

(22) (a) Pietro, W. J.; Francl, M. M.; Hehre, W. J.; Defrees, D. J.; Pople, J. A.; Binkley, J. S. *J. Am. Chem. Soc*. **1982**, *104*, 5039. (b) Dobbs, K. D.; Hehre, W. J. *J. Comput. Chem*. **1987**, *8*, 880.

(23) Binning, R. C.; Curtis, L. A. *J. Comput. Chem*. **1990**, *11*, 1206.

(24) Hay, P. J.; Wadt, W. R. *J. Chem. Phys*. **1985**, *82*, 299.

(25) Andrae, D.; Haeussermann, U.; Dolg, M.; Stoll, H.; Preuss, H. *Theor. Chim. Acta* **1990**, *77*, 123.

(26) (a) Wong, M. W.; Frisch, M. J.; Wiberg, K. B. *J. Am. Chem. Soc*. **1991**, *113*, 4776−4782. (b) Wong, M. W.; Wiberg, K. B.; Frisch, M. J. *J. Chem. Phys*. **1991**, *95*, 8991.

(27) (a) Wiberg, K. B.; Keith, T. A.; Frisch, M. J.; Murcko, M. *J. Phys. Chem*. **1995**, *99*, 9072. (b) Foresman, J. B.; Keith, T. A.; Wiberg, K. B.; Snoonian, J.; Frisch, M. J. *J. Phys. Chem*. **1996**, *100*, 16098.

(28) Peng, C.; Ayala, P. Y.; Schelegel, H. B.; Frisch, M. J. *J. Comput. Chem*. **1996**, *17*, 49

(29) (a) Casida, M. E.; Jamorski, C.; Casida, K. C.; Salahub, D. R. *J. Chem. Phys*. **1998**, *108*, 4439. (b) Stratmann, R. E.; Scuseria, G. E.; Frisch, M. J. *J. Chem. Phys*. **1998**, *109*, 8218.

(30) (a) Li, J.; Noodleman, L.; Case, D. A. In *Inorganic Electronic Structure and Spectroscopy*; Solomon, E. I., Lever, A. B. P., Eds.; Wiley: New York, 1999; Vol. I, Chapter 11, p 661. (b) Gorelsky, S. I.; Da Silva, S. C.; Lever, A. B. P.; Franco, D. W. *Inorg. Chim. Acta* **2000**, *300*−*302*, 698.

Table 1. Addition Rate Constants, Activation Parameters, and Corresponding ν_{NO}, $E_{NO^+/NO}$, and K_{eq} Values for Different $\{MX_5NO\}^n$

compd	k_{OH}[a] (M^{-1} s^{-1})	k_4[b] (s^{-1})	$\Delta H^{\ddagger}$ (kJ/mol)	$\Delta S^{\ddagger}$ (J/K mol)	$E_{NO^+/NO}$[c](V)	ν_{NO}[c] (cm^{-1})	K_{eq}[d] (M^{-2})
(**1**) *cis*-$[Ru(AcN)(bpy)_2NO]^{3+}$	$(5.60 \pm 0.07) \times 10^6$	2.31×10^6			0.35	1960	
(**2**) *cis*-$[Ru(bpy)(trpy)NO]^{3+}$	$(3.17 \pm 0.02) \times 10^5$	1.31×10^5	89 ± 1	159 ± 5	0.25	1946	2.1×10^{23} [10c]
(**3**) *cis*-$[Ru(bpy)_2(NO_2)NO]^{2+}$	$(5.06 \pm 0.02) \times 10^4$	2.75×10^4	83 ± 7	120 ± 20	0.18	1942	
(**4**) *cis*-$[Ru(bpy)_2ClNO]^{2+}$	$(8.5 \pm 0.1) \times 10^3$	4.6×10^3	100 ± 3	164 ± 8	0.05	1933	1.6×10^{15} [10e]
(**5**) *trans*-$[NCRu(py)_4CNRu(py)_4NO]^{3+}$	$(9.2 \pm 0.2) \times 10^3$	3.4×10^3	91 ± 4	135 ± 10	0.22	1917	3.2×10^{15} [12]
(**6**) *trans*-$[RuClNO(py)_4]^{2+}$	$(4.6 \pm 0.3) \times 10^1$	3.1×10^1	62 ± 1	-6 ± 5	0.09	1910	
(**7**) *trans*-$[Ru(NCS)NO(py)_4]^{2+}$	$(2.03 \pm 0.01) \times 10^2$	1.36×10^2			0.12	1902	
(**8**) *trans*-$[Ru(OH)NO(py)_4]^{2+}$	$(2.4 \pm 0.1) \times 10^{-1}$	1.6×10^{-1}			−0.22	1866	
(**9**) *trans*-$[Ru(NH_3)_4NO(pz)]^{3+}$	$(1.77 \pm 0.04) \times 10^2$	9.55×10^1	76 ± 2	54 ± 6	−0.11	1942	6.0×10^{8} [13]
(**10**) *trans*-$[Ru(NH_3)_4(nic)NO]^{3+}$	$(3.3 \pm 0.1) \times 10^1$	1.8×10^1	78 ± 1	44 ± 4	−0.18	1940	5.9×10^{7} [13]
(**11**) *trans*-$[Ru(Clpy)(NH_3)_4NO]^{3+}$	$(2.60 \pm 0.05) \times 10^1$	1.40×10^1			−0.19	1927	6.0×10^{6} [14]
(**12**) *trans*-$[Ru(NH_3)_4NO(py)]^{3+}$	$(1.45 \pm 0.02) \times 10^1$	7.82×10^0			−0.22	1931	2.2×10^{5} [13]
(**13**) *trans*-$[Ru(4\text{-}Mepy)(NH_3)_4NO]^{3+}$	$(9.54 \pm 0.06) \times 10^0$	5.14×10^0	75 ± 1	26 ± 4	−0.25	1934	7.7×10^{5} [14]
(**14**) *trans*-$[Ru(hist)(NH_3)_4NO]^{3+}$	$(7.6 \pm 0.4) \times 10^{-1}$	4.12×10^{-1}			−0.39	1921	4.6×10^{13} [13]
(**15**) $[Fe(CN)_5NO]^{2-}$	5.5×10^{-1} [8a]	3.9×10^0	53[8a]	−49[8a]	−0.29[15]	1945[8d]	1.5×10^{6} [8a]
(**16**) $[Ru(CN)_5NO]^{2-}$	9.5×10^{-1} [8c]	6.4×10^0	57[8c]	−54[8c]	−0.35[15]	1926[8d]	4.4×10^{6} [8c]
(**17**) $[Os(CN)_5NO]^{2-}$	1.37×10^{-4} [8d]	8.63×10^{-4}	80[8d]	−73[8d]	−0.68[15]	1897[8d]	4.2×10^{1} [8d]

[a] Derived from the rate law. [b] Obtained through $k_4 = k_{OH}/K_{ip}$, with K_{ip} being estimated according to an electrostatic model (see Experimental Section). [c] This work. [d] Values obtained from the literature.

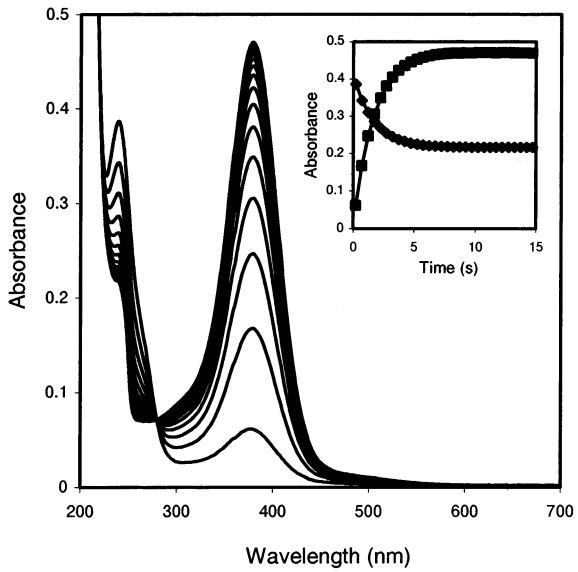

Figure 1. Kinetic study for the reaction of *trans*-$[Ru(4\text{-}Mepy)(NH_3)_4(NO)]^{3+}$ with OH^-. $I = 1$ M (NaCl); $T = 35.0$ °C; $[OH^-] = 0.015$ M; [complex] $= 4 \times 10^{-6}$ M; cycle time = 0.5 s. Inset: Plots of absorbance vs time at 378 (■) and 240 nm (♦).

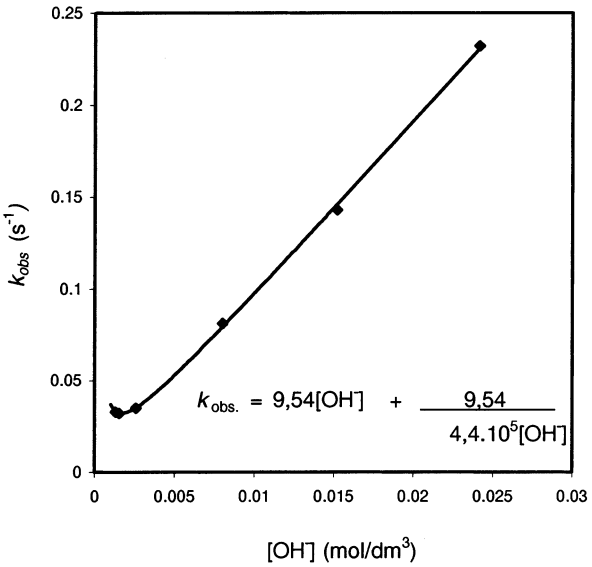

Figure 2. Dependence of k_{obs} on $[OH^-]$ for *trans*-$[Ru(4\text{-}Mepy)(NH_3)_4(NO)]^{3+}$. $T = 25.0$ °C; $I = 1$ M (NaCl).

shows that a clean conversion occurs. The reaction is reversed, to give the reactants, upon acidification. These general features are repeated for all the similar conversions of the complexes of Table 1.

The increase and decrease of the absorbance traces for the preceding reaction, at 378 and 240 nm, respectively, are displayed at the inset of Figure 1. They agree with a pseudo-first-order behavior, up to at least three half-lives. Figure 2 shows the plot of k_{obs} against the concentration of OH^-, which can be represented by

$$k_{obs} = a[OH^-] + b/[OH^-] \quad (2)$$

An expression of the same form has been derived for k_{obs},[8b,d] assuming the following general mechanistic scheme:

$$[MX_5NO]^n + OH^- \rightleftharpoons \{[MX_5NO]^n \cdot OH^-\} \quad K_{ip} \quad (3)$$

$$\{[MX_5NO]^n \cdot OH^-\} \rightleftharpoons [MX_5NO_2H]^{(n-1)} \quad K_4, k_4, k_{-4} \quad (4)$$

$$[MX_5NO_2H]^{(n-1)} + OH^- \rightleftharpoons [MX_5NO_2]^{(n-2)} + H_2O \quad K_5 \quad (5)$$

Equations 3−5 include a fast ion pair formation preequilibrium, eq 3, prior to the relevant nucleophilic addition step, eq 4. The latter leads to the $[MX_5NO_2H]^{(n-1)}$ intermediate, which may go back to the reactants or react as in eq 5 to form the final product.[8] The values of K_{ip} (M^{-1}) were estimated by using electrostatic models[17] (see Experimental Section). The values of *a* and *b* in eq 2 can be traced to $a = k_{OH^-}$ and $b = k_{OH^-}/K_{eq}$, with $k_{OH^-} = K_{ip}k_4$ and $K_{eq} = K_{ip}K_4K_5$.[8d] Thus, values of k_{OH^-} (M^{-1} s^{-1}) as well as of K_{eq} (M^{-2}) can be obtained, although the latter may be measured more accurately by independent equilibrium measurements. For most of the reactions (when $[OH^-]$ and K_{eq} are sufficiently high), the influence of the $k_{OH^-}/K_{eq}[OH^-]$ term is negligible, and k_{OH^-} may be obtained from the slope of the plot of k_{obs} against $[OH^-]$. Then, the value of k_4 (s^{-1}),

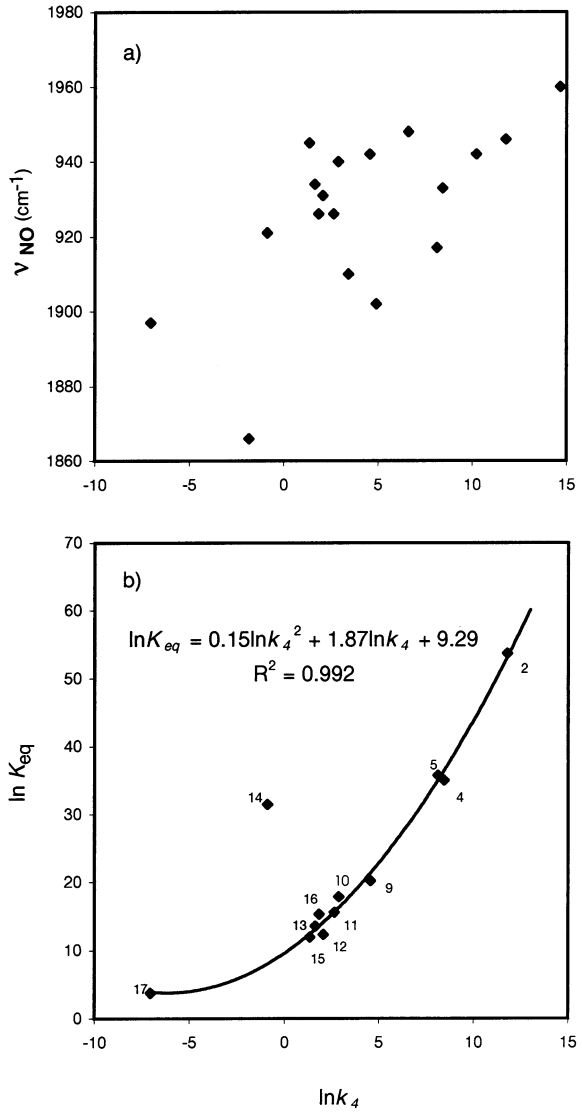

Figure 3. Plots of (a) ν_{NO} and (b) ln K_{eq}, against the nucleophilic rate constant, ln k_4. See Table 1 for the assignment of numbers.

corresponding to the elementary step for nucleophilic addition, can be calculated using estimated values of K_{ip} (see Table 1).[8d]

Figure 3a shows a correlation between ln k_4 against ν_{NO}, with a high dispersion in the intermediate region. Indeed, ν_{NO} is an uncertain parameter for predicting the electrophilic reactivity of a given nitrosyl complex. Figure 3b shows also a correlation (not linear but quadratic) between ln k_4 and ln K_{eq}, giving some justification to the current use of K_{eq} as an indicator of nucleophilic reactivity.[31]

Figure 4 shows a plot of ln k_4 against $E_{NO^+/NO}$. A very good correlation is obtained ($r^2 = 0.993$) for most of the complexes studied, with the exception of those corresponding to the *trans*-$[Ru(py)_4(X)NO]^{n+}$ series, which lay in a parallel line, showing lower rates than expected.[32] The slope of the main line is 20.2 V^{-1}. Remarkably, the correlation spans

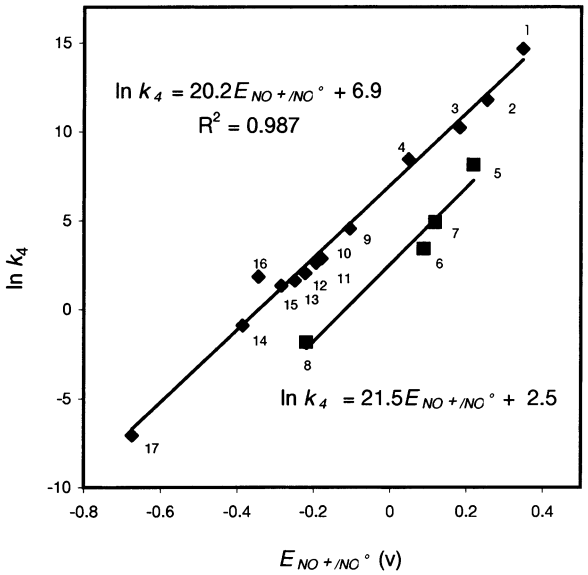

Figure 4. LFER plot of ln k_4 against $E_{NO^+/NO}$ for the reactions of a series of $\{MX_5NO\}^n$ complexes with OH^-. See Table 1 for the assignment of numbers.

around 10 orders of magnitude in the values of k_4, covering a range of around 1 V in the redox potentials.

Figure 4 is a linear free-energy relation (LFER), as frequently found in the correlations of kinetic versus thermodynamic parameters for a set of reactions governed by the same mechanism.[33] The value of the slope is close to the one predicted for LFERs in weakly coupled outer-sphere one-electron-transfer reactions (-19.4 V^{-1} or $-0.5/RT$) following Marcus' treatment for cross reactions.[34,35] Marcus extended the theory to atom-transfer reactions, with the prediction that a slope of 0.5 in the plot of ΔG^* versus $\Delta G°$ could also be found in the case of substitution reactions proceeding through an associative mechanism.[36] The appearance of such an LFER for an addition reaction as described by eqs 3−5 is, to our knowledge, a first situation found in mechanistic inorganic chemistry. The result is consistent with an increase in coordination number for the N atom in nitrosyl, with a formal change in hybridization from linear M−N−O to angular $M-NO_2H$, supporting an associative route (see DFT calculations).

Figure 5 shows the trends in the activation parameters for the reactions of complexes in Table 1.

(31) Complex **14** has been reported with a strikingly high value of K_{eq}. This is probably due to perturbing acid−base equilibria associated with the histidine ligand. On the other hand, both redox potential and rate constant values are consistent with the linear correlation shown in Figure 4.

(32) Steric hindrance is probably a main reason for tetrapyridine complexes **5**−**8** falling out of the correlation between ln k_4 versus E, with a lower rate than predicted. In these complexes, the pyridines are free to rotate, and they are expected to favor a staggered configuration. In this position, the H points to the NO group, leaving less space to be attacked by OH^- (cf. Coe, B. J.; Meyer, T. J.; White, P. S. *Inorg. Chem.* **1995**, *34*, 593)). For other complexes, the coligands are smaller, or they are fixed in a planar configuration (polypyridines).

(33) (a) Edwards, J. O. *Inorganic Reaction Mechanisms*; W. A. Benjamin, Inc.: New York, 1965. (b) Swaddle, T. W. *Coord. Chem. Rev.* **1974**, *14*, 217. (c) Swaddle, T. W. *Advances in Inorganic and Bioinorganic Mechanisms, Vol. 2*; A. G. Sykes, Ed.; Academic Press: London, 1983; p 95.

(34) (a) Marcus, R. A. *J. Phys. Chem.* **1963**, *67*, 853, 2889. (b) Sutin, N. *Annu. Rev. Phys. Chem.* **1966**, *17*, 119.

(35) (a) Oliveira, L. A. A.; Giesbrecht, E.; Toma, H. E. *J. Chem. Soc., Dalton Trans.* **1979**, 236. (b) Parise, A. R.; Baraldo, L. M.; Olabe, J. A. *Inorg. Chem.* **1996**, *35*, 5080.

(36) (a) Marcus, R. A. *J. Phys. Chem.* **1968**, *72*, 891. (b) Cohen, A. O.; Marcus, R. A. *J. Phys. Chem.* **1968**, *72*, 891.

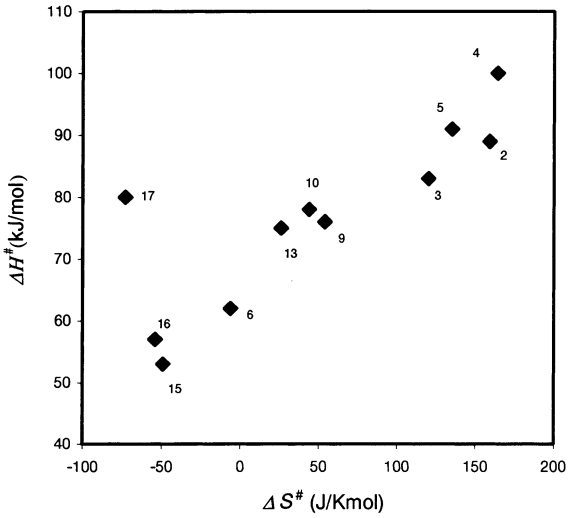

Figure 5. Plot of the activation enthalpies against the activation entropies for the reactions of $\{MX_5NO\}$ complexes with OH^- (see Table 1).

The increase in rate constants and redox potentials goes in parallel with an *increase* in *both* the activation enthalpies and entropies. On this basis, the reactions appear as entropically driven. While the trends in the entropies can be reasonably explained considering the different solvational changes related to the reactions of species carrying equal or opposite charges,[37] the consideration of enthalpy changes is not so straightforward. We propose that the rate of addition in eq 4 should be controlled mainly by the energetically costly steps involving the reorganization of the linear MNO moiety to angular $M-NO_2H$, as anticipated previously.

Computational Results. (i) Influence of the Coligands on the Reactivity. Although the UV−vis spectral results account for the reversible formation of $[MX_5NO_2]^{(n-2)}$ in eq 1, direct evidence on the proposed $[MX_5NO_2H]^{(n-1)}$ intermediate formation, eq 4, is not available. This is a general situation in the studies of electrophilic reactions of bound nitrosyl, where the claimed adduct-intermediates react usually very fast. Sometimes the spectral evidence suggests their transient existence, as in the case of thiolates,[38] but an appropriate characterization is generally lacking. Quantum chemical calculations become helpful for the characterization and stability analysis of the adduct-intermediates. On the other hand, they allow us to better understand the correlations experimentally found that are presented in this article. With this in mind, we have analyzed representative members of the set of $\{MX_5NO\}^n$ complexes, associated with different values of ln *k*, namely complexes **1**, **2**, **4**, **12**, **15**, and **16** (Table 1). We have mainly focused the attention on reactants and products of reactions 3 and 4, respectively.

Geometry optimization shows that the reactants and products are true minima in the potential hypersurface, with no negative components in the calculated Hessian. The optimized geometries are shown in Figure 6 for representative examples.

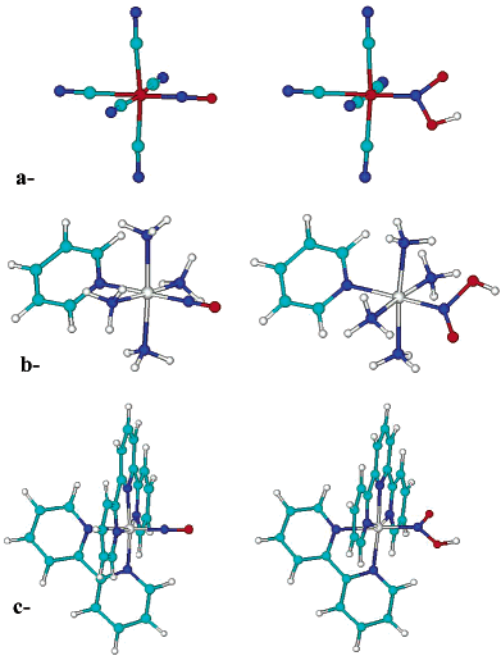

Figure 6. Geometries optimized at the B3LYP/6-31G** level (SDD pseudopotentials on the metal centers) for representative members of the set (nitrosyls and OH^- addition products): (a) $[Fe(CN)_5NO]^{2-}$; (b) *trans*-$[Ru(NH_3)_4NO(py)]^{3+}$; (c) *cis*-$[Ru(bpy)(trpy)NO]^{3+}$.

The geometrical parameters for the groups more strongly involved in the reaction (MNO, MNO_2H) are given in Table 2 (see also Table SI 1 in the Supporting Information). The information in these tables comprises the structural data obtained with the different basis sets used throughout the calculations. Also included are the calculated charges on the electrophilic centers. Comparisons are made with consideration of the N atom, the NO group, or the MNO group for an accurate definition of the electronic characteristics of this center. Local charges on the atomic centers are only considered in their trend within the series as they belong to a Mulliken population partition analysis.

Using the 3-21G basis (Table SI 1), an increase in the rate constant correlates with an increase of the charge on the N atom, a decrease in the NO distance, and a simultaneous increase in the M−N one. Within a pseudopotential approach, the simultaneous consideration of Fe and Ru derivatives does not lead to a good correlation of the above-mentioned parameters with ln *k* (Table 2). When only Ru complexes are considered, the trend of the variation of ln *k* with the structural parameters resembles the one previously described for the case where the 3-21G basis were used. Correlation with the charge needs to consider the charge on the NO group instead of the charge on the N atom alone. Moreover, further addition of the M center, to define a group charge q_{MNO}, allows one to include even NP to attain a trend of variation of ln *k* qualitatively correlated with it. This fact offers a clear demonstration that the major influence on the rates of the electrophilic reactions is exerted by the ancillary coligands, a result that should be emphasized, even despite being a reasonably predictable one. This qualitative correla-

(37) (a) Wilkins, R. W. *Kinetics and Mechanism of Reactions of Transition Metal Complexes*, 2nd ed.; VCH: Weinheim, 1991. (b) In Figure 5, the osmium cyano complex deviates from the correlation because the low rate is associated mainly with an enthalpy effect. Activation entropy changes are similar for the three pentacyanonitrosylmetalates.[8d]

(38) (a) Johnson, M. D.; Wilkins, R. G. *Inorg. Chem.* **1984**, *23*, 231. (b) Schwane, J. D.; Ashby, M. T. *J. Am. Chem. Soc.* **2002**, *124*, 6822.

Table 2. Structural and Electronic Parameters Derived from Calculations Using Pseudopotentials for the Metal Centers[a]

		d_{M-N}	d_{N-O}	$d_{N-O(H)}$	∠MNO	∠ONO	q_N	q_{NO}	q_{MNO}	ν_{NO}
$[Ru(AcN)(bpy)_2NO]^{3+}$	LAN	1.806	1.134		178.2		0.128	0.138	1.148	1993
	SDD	1.778	1.137		178.6		0.207	0.127	1.112	1981
$[Ru(AcN)(bpy)_2NO_2H]^{2+}$	SDD	1.994	1.203	1.389	128.0	114.2				
$[Ru(bpy)(trpy)NO]^{3+}$	LAN	1.799	1.137		175.3		0.108	0.101	1.131	1974
	SDD	1.772	1.141		176.2		0.176	0.082	1.115	1964
$[Ru(bpy)(trpy)NO_2H]^{2+}$	SDD	1.991	1.204	1.391	128.4	114.3				
$[Ru(bpy)_2ClNO]^{2+}$	LAN	1.786	1.139		172.7		0.136	0.106	0.779	1969
	SDD	1.759	1.143		175.5		0.182	0.058	0.779	1959
$[Ru(bpy)_2ClNO_2H]^{+}$	SDD	1.965	1.207	1.405		114.4				
$[RuA_4NO(py)]^{3+}$ *b*	LAN	1.825	1.129		180.0		0.165	0.094	0.847	2005
	SDD	1.792	1.133		180.0		0.213	0.081	0.899	1983
$[RuA_4NO_2H(py)]^{2+}$ *b*	SDD	1.952	1.209	1.394	128.6	114.7				
$[Ru(CN)_5NO]^{2-}$	LAN	1.779	1.163		180.0		0.004	−0.215	−0.067	1874
	SDD	1.758	1.164		180.0		0.105	−0.201	−0.169	1871
$[Ru(CN)_5NO_2H]^{3-}$	SDD	1.969	1.225	1.464	133.1	108.7				
$[Fe(CN)_5NO]^{2-}$	LAN	1.618	1.157		180.0		0.222	−0.026	−0.576	1906
	SDD	1.617	1.158		180.0		0.197	−0.063	−1.327	1901
$[Fe(CN)_5NO_2H]^{3-}$	SDD	1.833	1.224	1.457	132.9	108.6				

[a] Distances (*d*) in angstroms; angles in degrees. q_N: calculated charge on the N atom of the NO group. q_{NO}: calculated charge on the NO group. q_{MNO}: calculated group-charge. See text for details. [b] A = amine.

tion presents a discontinuity for $[Ru(NH_3)_4NO(py)]^{3+}$. According to the calculated structural and electronic data, a larger value of ln *k* should have been measured for these compounds. It is likely that the acceptor interactions of the NH_3 ligands with water may severely influence their coordination ability toward the metal and therefore the electronic density on the nitrosyl. These specific donor−acceptor interactions have been thoroughly discussed and theoretically demonstrated for the $[Ru(NH_3)_5py]^{2+}$ complexes.[39]

Bonding of the NO ligand in six-coordinated $\{MX_5NO\}^n$ nitrosyls has been explained through the stabilization of the π^*_{NO} orbital due to bonding interactions with the metal d orbitals. Antibonding interactions between the same orbitals turn out to define the LUMO in the molecule.[5,40] Back-donation to the antibonding orbital determines the N charge and NO interatomic distance. Because this effect is smaller for the coligands more characterized as acceptors, both the electron density and the NO distance decrease when going from cyano- to the polypyridine coligands.

An MO analysis shows that the antibonding LUMO of the nitrosyl complexes, with a large contribution of the π^*_{NO}, is largely delocalized over the M centers. This description, which is in agreement with previous interpretations of the bonding in six-coordinated metal nitrosyls,[5,40] holds for the different levels of theory that have been considered. Thus, the definition of a group charge becomes more reliable, giving strong support to the correlation with ln *k*. The same MO analysis shows that the HOMO, strongly localized on the metal in the pentacyanonitrosyl complexes, spreads over the ligands in the polypyridine systems, decreasing the electronic density on the electrophilic group.

It is worth mentioning that the energy involved in reaction 4 (ΔE = energy of the products − energy of the reactants) is negative for the cases associated with positive values of ln *k*, and positive in all the other cases (Table 3). This indicates that the addition product of reaction 4, far from being only a stable intermediate, is in several cases more stable than the reactants. Keeping aside for the moment $[Ru(NH_3)_4NO(py)]^{3+}$, the trend in ΔE variation correlates with the observed trend in ln *k*. A possible explanation may follow from the fact that larger ln *k* values also correlate with lower energy values of the calculated LUMOs. Reaction 4 can be formally described as a nucleophilic attack of OH^- to the linearly coordinated nitrosyl. Occupation of one of the degenerate e (mainly π^*_{NO}) LUMO orbitals splits their energy, lowering the symmetry from C_4v to C_s. Bond formation is associated with the interaction of the p orbital of OH^-, mainly centered on the O atom, with the π^*_{NO} stabilized after splitting. The NO distance increases, then, for all the members of the series (Table 2). In this process, a lower energy of the LUMO favors the stabilization of OH^-, an effect that is reflected in larger negative ΔE values. The energy of the LUMO becomes, then, an important determinant of the energy involved in this process. The variation in the ONO and MNO planar angles along the members of the series shows that a geometry closest to that imposed by an sp^2 hybridization of the N atom is attained for the stronger stabilization of the OH^--addition product. The linear → bent reorganization corresponds formally to the conversion of an

Table 3. Energy Differences between Products and Reactants (eq 4), ΔE, and Energies of the Nitrosyl LUMOs, E_{LUMO}, for Selected Complexes[a]

	ΔE (eV)		E_{LUMO}(au)		
	3-21G	SDD	3-21G	SDD	SDD-solv
$[Ru(AcN)(bpy)_2NO]^{3+}$	−16.52	−0.55	−0.50	−0.47	−0.176
$[Ru(bpy)(trpy)NO]^{3+}$	−16.29	−0.53	−0.48	−0.46	−0.166
$[Ru(bpy)_2ClNO]^{2+}$	−13.01	−0.41	−0.36	−0.35	−0.164
$[Ru(NH_3)_4NO(py)]^{3+}$	−18.22	−0.64	−0.56	−0.55	−0.161
$Ru(CN)_5NO]^{2-}$	1.37	0.099	0.134	0.129	−0.145
$Fe(CN)_5NO]^{2-}$	2.06	0.096	0.165	0.135	−0.122

[a] Last column shows the results when the effect of the solvent was considered in the calculations.

(39) (a) Chen, P.; Meyer, T. J. *Chem. Rev.* **1998**, *98*, 1439. (b) Stavrev, K.; Zerner, M. C.; Meyer, T. J.; *J. Am. Chem. Soc.* **1995**, *117*, 8684.
(40) Westcott, B. L.; Enemark, J. H. In *Inorganic Electronic Structure and Spectroscopy, Vol. II*; Solomon, E. I., Lever, A. B. P., Eds.; Wiley-Interscience: New York, 1999; Chapter 7, p 403.

Table 4. Selected Distances (Å), Angles (deg), and IR Stretching Frequencies (ν, cm^{-1}) Calculated for the Different Steps of Reaction 1, at the B3LYP/6-31G** Level with Experimental Values Given When Available (X = $[Fe(CN)_5]$)

	$[XNO]^{2-}$(exp)[a]	$[XNO]^{2-}$	TS[b]	$[XNO_2H]^{3-}$	$[XNO_2]^{4-}$
d_{FeC} ax	1.9257(9)	1.9694	1.9878	1.9888	1.987
d_{FeC} eq[c]	1.935	1.9595	1.9890	1.9880	2.011
d_{FeN}	1.6656(7)	1.6155	1.8223	1.813	2.104
d_{CN} ax	1.1591(12)	1.1683	1.1751	1.1755	1.184
d_{CN} eq[c]	1.1613	1.1691	1.1761	1.1782	1.1826
d_{NO}	1.1331(10)	1.1604	1.2255	1.2275	1.2642
d_{NO}(H)			1.4536	1.4713	1.2642
d_{OH}			0.9801	0.9784	
∠FeNO	176.03(7)	179.96	134.69	133.11	122.48
∠ONO			109.25	107.98	115.02
∠CFeC eq[d]	176.63(4)	180.00		173.5	179.83
ν_{CN} (s)	2147−2177	2161−2170		2100−2120	2043
ν_{NO} (s)	1943	1907		1567, 1266, 789	1317, 1351, 802
ν_{Fe-N} (s)	658	712		575	574

[a] Reference 45. [b] Transition state. [c] The fourth digit averaged. [d] *trans*-Cyanides.

{MNO}^{6} species into an {MNO}^{8} one, in the Enemark−Feltham notation.[5]

Solvent models allow us to consider the effects that the environment exerts on the different coligands, and the way it influences the reactivity of the complexes. Cyano ligands decrease their electron density through donor interactions with the solvent, an effect that is reflected in the LUMO, mainly localized on the MNO moiety. The calculated energy of the LUMO becomes lower, and this orbital becomes, thus, stabilized. The other ligands, on the other hand, increase their electron density when interacting with water, destabilizing the LUMO. The influence of the solvent is more sizable for $[Ru(NH_3)_4NO(py)]^{3+}$, with a larger shift in the energy of the associated LUMO. This explains why, within this approach, $[Ru(NH_3)_4NO(py)]^{3+}$ can be also included in a correlation of the LUMO with ln *k* (Table 3). A discrete solvent model, with water molecules coordinated to the NH_3 moieties, would probably allow a better fit.[39b]

The comparison of the structural parameters calculated with different basis sets shows that the NO distance d_{NO} is overestimated when the 3-21G basis are used (Table SI 1). The pseudopotentials that have been considered give values very much closer to those from the experiment. Both LANL2DZ and SDD show very similar results (Table 2). The overestimation of the NO distance has been previously analyzed by Gorelsky and Lever,[41] using a similar calculation level, and also by Boulet et al.[42] and Wanner et al.,[43] using the ADF program. According to the data of ref 41, it seems that triple-ζ basis sets including diffuse and polarization functions are necessary for a closer approximation to the experimental d_{NO} value. This analysis does not necessarily hold for the complexes bearing N-heterocyclic ligands (py, bpy, trpy). Experimental data reported for $[Ru(AcN)(bpy)_2(NO)]^{3+}$ (d_{Ru-NO} = 1.710 Å, d_{NO} = 1.148 Å)[44] are in close agreement with our calculated data, giving confidence to our calculation for complexes with these substituents.

Experimental frequencies for the pentacyanonitrosyl complexes are in good agreement with those previously reported (ref 41 and refs therein). Keeping aside $[Ru(NH_3)_4NO(py)]^{3+}$, the calculated frequencies are underestimated by 30 cm^{-1} for the complexes with polypyridine coligands, and by 50 cm^{-1} for the pentacyano ones. The trend of increase of ν_{NO} with increasing reactivity, experimentally found, is reproduced in the calculations. According to the results reported by Gorelsky and Lever,[41] the mismatching of either 50 cm^{-1} or 30 cm^{-1} should not be associated with a solvent effect, but with the size of the basis.

(ii) Calculated Reaction Mechanism for NP. The complete reaction profile has been analyzed for NP including polarization functions in the basis. Structural parameters and spectroscopic data are given in Table 4 for the different steps of the reaction. Experimental values are included when available.[45]

From the comparison of Tables SI 1 and 4, it becomes evident that the effect of the basis is mainly reflected in the NO distance, which decreases when polarization functions are considered in the calculations. Better values are obtained, however, when pseudopotentials are used for the Fe atom (Table 2). The overall increase of the bond lengths for $[Fe(CN)_5NO_2H]^{3-}$, compared to NP, suggests an increase in the electron population in the antibonding system, delocalized over the metal and the ligands, similar to the one previously found when the two-electron reduction of NP to $[Fe(CN)_5HNO]^{3-}$ was theoretically analyzed.[46]

The energy of the OH^--addition product is calculated 0.12 au higher than the energy of the reactants. The energy of the TS is also higher, by 0.123 au, and very close to the product of step 4 (Figure 7). The main structural difference between TS and product is related to the value of the FeNOH torsion angle, 164.35° in the TS, versus 179.99° in the

(41) Gorelsky, S. I.; Lever, A. B. P. *Int. J. Quantum Chem*. **2000**, *80*, 636.
(42) Boulet, P.; Buchs, M.; Chermette, H.; Daul, C.; Gilardoni, F.; Rogemond, F.; Schlapfer, C. W.; Weber, J. *J. Phys. Chem. A* **2001**, *105*, 8991.
(43) Wanner, M.; Scheiring, T.; Kaim, W.; Slep, L. D.; Baraldo, L. M.; Olabe, J. A.; Zális, S.; Baerends, E. J. *Inorg. Chem*. **2001**, *40*, 5704.
(44) Nagao, H.; Ito, K.; Tsuboya, N.; Ooyama, D.; Nagao, N.; Howell, F. S.; Mukaida, M. *Inorg. Chim. Acta* **1999**, *290*, 113.
(45) (a) Carducci, M. D.; Pressprich, M. R.; Coppens, P. *J. Am. Chem. Soc*. **1997**, *119*, 2669. (b) Chacón Villalba, M. E.; Guida, J. A.; Varetti, E. L.; Aymonino, P. J. *Spectrochim. Acta* **2001**, *A57*, 367.
(46) González Lebrero, M. C.; Scherlis, D. A.; Estiú, G. L.; Olabe, J. A.; Estrin, D. A. *Inorg. Chem*. **2001**, *40*, 4127.

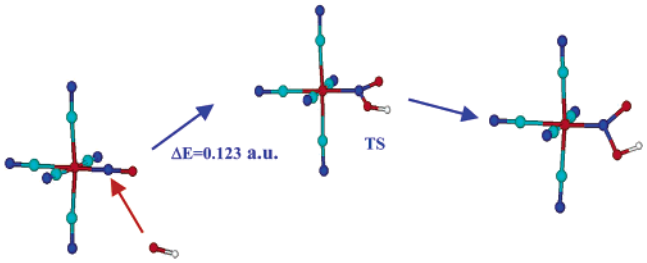

Figure 7. Optimized geometries for the initial steps of the reaction of NP with OH^-. More details are available in the text.

addition product $[Fe(CN)_5NO_2H]^{3-}$. According to these data, the energy involved in the evolution from TS to the intermediate adduct is mainly associated with the change in hybridization of the O atom, from sp^3 in the OH^- ion to sp^2 in the coordinated adduct. The energy cost when going from reactants to TS is largely associated with the electronic reorganization of the N atom. A similar TS structure has been found using 3-21G basis. However, another TS has also been identified at this level, with an energy 0.066 au higher than the previously described one. In this structure, the OH^- ligand is not close enough to the nitrosyl to induce a change in its hybridization. We have disregarded this structure because of the low quality of the 3-21G basis.

Table 4 shows some selected frequencies for the calculated species. The values for NP are in agreement with those calculated when pseudopotentials were used for Fe (Table 2). Although underestimated relative to our experimental data, they show coincidence with previous experiments, and also with previous theoretical results.[46] For $[M(CN)_5NO_2]^{4-}$, the values at 1351, 1317, and 802 cm^{-1} are consistent with stretchings and deformations of the nitro group, as found in transition metal related complexes.[47] The value at 2043 cm^{-1} can be assigned to the ν_{CN} stretching, typical of M(II) pentacyano complexes with moderately π-accepting sixth L ligands,[48] in contrast with the high values for NP, at ca. 2160 cm^{-1}. The ν_{FeN} stretching has a lower value than for NP, as expected for a weaker Fe−N bond. The frequencies for the $[M(CN)_5NO_2H]^{3-}$ intermediate strongly support the protonation of the nitro group. One of the nitro stretchings appears as highly upshifted, 1567 cm^{-1}. A shift of similar magnitude has been found for dinuclear Co(III) complexes bridged by the nitro group.[47] In the absence of IR data for NO_2H ligands,[47] we can reasonably compare the protonation process with the binding of the exposed oxygen atom of the nitro group to another Co(III). On the other hand, the stretching at 1266 cm^{-1} has a large participation of H, interacting with both O atoms and N, whereas the one at 789 cm^{-1} mainly involves the doubly bonded NO and H, consistent with a deformation mode of the NO_2H group. A similar frequency pattern has been calculated for the other adducts, using pseudopotentials on the M centers. The previous interpretation can be also applied to these cases.

Electronic transitions have been calculated within a TDDFT approach. The results are remarkably good when dealing with excited states of valence type but may be affected by incorrect asymptotic behavior of the potential when excitations involve transitions to unbound orbitals, as is the case of the anions that we are analyzing. However, the results obtained for NP are in good agreement with the experimental data, increasing our confidence in the results for the other species, which are, at present, a prediction. We calculate MLCT transitions for NP at 2.34 eV ($f = 2 \times 10^{-4}$), 3.45 eV ($f = 29 \times 10^{-4}$), and 3.80 eV ($f = 42 \times 10^{-4}$). This is in good agreement with experiment, which locates the transitions at 2.49, 3.15, and 3.76 eV.[49] Recent calculations using the generalized gradient approximation and the B88P86 functional, within the ADF99 program package, reported values at 1.91, 3.36, and 3.94 eV, respectively.[42] The lowest excitation corresponds to a transition from the HOMO (d_{xy}) to the LUMO. Lower energy occupied orbitals are involved in the higher energy transitions. An intense MLCT band at 3.26 eV (380 nm, $f = 0.11$) is calculated for $[M(CN)_5NO_2H]^{3-}$, also associated with $d \rightarrow \pi^*_{NO}$ transitions, together with bands of lower intensity at 2.34 eV ($f = 0.0013$), 2.76 eV ($f = 0.0014$), and 2.95 eV ($f = 0.001$). Bands at 3.51 eV (352 nm, $f = 0.04$) and 3.15 eV (393 nm, $f = 0.01$) are calculated for the $[M(CN)_5NO_2]^{4-}$ ion. They are associated with d_π(HOMO) $\rightarrow \pi^*_{NO2}$(LUMO) transitions and compare fairly well with the experimental value found at 400 nm ($\epsilon = 3000$ M^{-1} cm^{-1}).[50] The transition of lower intensity has mixed contributions of d−d transitions.

Conclusions

From the simultaneous consideration of our experimental and theoretical data, we propose that the rate of addition in eq 4 should be controlled mainly by the energetically costly steps involving the reorganization of the linear MNO moiety to angular $M-NO_2H$, as well as the geometry changes ascribed to the OH^- reactant upon coordination (see previous description). Moreover, we expect a stronger stabilization of the MNO moieties for complexes receiving a smaller back-bonding interaction arising from the coligands. Back-bonding to the antibonding LUMO, increasing the electronic density of this orbital, decreases the bond order. Bond reorganization becomes favored, and the activation enthalpy decreases. For the complexes at the top of Table 1, showing a higher triple bond character, bond reorganization is disfavored, and the reaction is more endothermic. The larger triple bond character is confirmed by the smaller calculated NO distance and larger calculated ν_{NO} value. Calculated energies (Table 3) are based on the difference between the addition products of reaction 4 and the reactants of reaction 3, prior to ion pair formation. For this process, an increase in the rate constant parallels the decrease of the total energy. The influence of the MNO density charge in the ion pair stabilization is included. These ΔE values, together with the charge on the electrophilic center, q_{MNO}, and E_{LUMO}, appear as valuable descriptors of the reactivity of the complexes.

(47) Nakamoto, K. *Infrared and Raman Spectra of Inorganic and Coordination Compounds*, 4th ed.; Wiley: New York, 1986.
(48) Macartney, D. H. *Rev. Inorg. Chem.* **1988**, *9*, 101.
(49) (a) Manoharan, P. T.; Gray, H. B. *J. Am. Chem. Soc.* **1965**, *87*, 3340. (b) Manoharan, P. T., Gray, H. B. *Inorg. Chem.* **1966**, *5*, 823.
(50) Maciejowska, I.; Stasicka, Z.; Stochel, G.; van Eldik, R. *J. Chem. Soc., Dalton Trans.* **1999**, 3643.

It is easily understandable how the charge on the electrophilic center influences the first step of preequilibrium, associated with K_{ip}, which is mainly an electrostatic process, with a probable positive contribution to the total enthalpy. A closer approach between the centers of opposite charge in the outer-sphere complex favors the charge-transfer to the LUMO, triggering the onset of reaction 4. Despite this contribution, the endothermic nature of step 4 is related, as previously mentioned, to the electronic reorganization of the NO ligand. Therefore, although the stabilization of the OH^- by interaction with the LUMO favors the next step of the reaction (reaction 4), this step is more energetically demanding, resulting in an endothermic process associated with k_4. This effect is more important the larger the triple bond character of NO is. A calculated entropy would always render a negative value because of the loss of the translational contribution of the OH^- in the first step of ion pair formation. We rely, for these data, on the experimentally measured values.

In summary, a detailed experimental and theoretical picture has been shown for an important reaction in coordination chemistry, namely the nucleophilic addition of OH^- to a broad set of nitrosyl complexes. By measuring the relevant rate constants and activation parameters, along with the spectroscopic and electrochemical information sensing the variable electronic densities at the {MNO} moieties, we could place this reaction type under rigorous scrutiny. The results may be compared with those found for the reactions comprising additions of bases to bound carbonyl,[51] and also with the general situation in organic chemistry, where the variable electrophilicities at carbon must be afforded in terms of empirical parameters dealing with substituent effects.[52] The LFER covers an impressive range of rates and redox potentials, showing that it is a useful predictive tool. The interpretation of activation parameters suggests that both electronic and solvation effects influence the nucleophilic reaction rates. Theoretical calculations played a relevant role in the interpretation of the different factors influencing the reactivity, offering also electronic descriptors of predictive value. The analysis could seemingly be extended to other nucleophiles, and this is important for the predictions having a more general validity. Although different rates are operative for a given complex by changing the nucleophile, we should expect similar trends for any nucleophile considering the $\{MX_5NO\}$ series, if the relevant rate constants do reflect the adduct-formation step, with the ensuing decompositions going faster. Our results for the reactions of nitrogen hydrides with the pentacyanonitrosylmetalate ions seem to confirm this general kinetic behavior.[53]

Acknowledgment. We thank the Universities of Buenos Aires and La Plata, the National Scientific Council (Conicet), the Agency for Science Promotion (ANPCyT), the VolkswagenStiftung, and FAPESP (Brazil) for financial support. G.L.E. and J.A.O. are members of the scientific staff of Conicet, and F.R. is a fellow of the same Institution. M.E.R. was a postgraduate student at IQSC (Sao Carlos, USP).

Supporting Information Available: Table SI 1, showing structural and electronic parameters for selected $\{MX_5NO\}^n$ and $\{MX_5NO_2H]^{n-1}$, calculated at a B3LYP/3-21G level. This material is available free of charge via the Internet at http://pubs.acs.org.

IC025653Q

(51) Ford, P. C.; Rokicki, A. *Adv. Organomet. Chem*. **1988**, *28*, 139.

(52) March, J. *Advanced Organic Chemistry*, 4th ed; Wiley: New York, 1992.

(53) Gutiérrez, M. M.; Amorebieta, V. T.; Estiú, G. L.; Olabe, J. A. *J. Am. Chem. Soc*. **2002**, *124*, 10307. (b) Olabe, J. A.; Estiú, G. L., submitted for publication.